

EstrellaNueva: an open-source software to study the interactions and detection of neutrinos emitted by supernovae

O. I. GONZÁLEZ-REINA,¹ J. RUMLESKIE,² AND E. VÁZQUEZ-JÁUREGUI¹

¹*Instituto de Física, Universidad Nacional Autónoma de México, A.P. 20-364, Ciudad de México 01000, México*

²*Laurentian University, Department of Physics, 935 Ramsey Lake Road, Sudbury, ON P3E 2C6, Canada*

ABSTRACT

Supernovae emit large fluxes of neutrinos which can be detected by detectors on Earth. Future tonne-scale detectors will be sensitive to several neutrino interaction channels, with thousands of events expected if a supernova emerges in the galaxy neighborhood. There is a limited number of tools to study the interaction rates of supernova neutrinos, although a plethora of available supernova models exists. EstrellaNueva is an open-source software to calculate expected rates of supernova neutrinos in detectors using target materials with typical compositions, and additional compositions can be easily added. This software considers the flavor transformation of neutrinos in the supernova through the adiabatic Mikheyev–Smirnov–Wolfenstein effect, and their interaction in detectors through several channels. Most of the interaction cross sections have been analytically implemented, such as neutrino-electron and neutrino-proton elastic scattering, inverse beta decay, and coherent elastic neutrino-nucleus scattering. This software provides a link between supernova simulations and the expected events in detectors by calculating fluences and event rates to ease any comparison between theory and observation. It provides a simple and standalone tool to explore many physics scenarios offering an option to add analytical cross sections and define any target material.

1. INTRODUCTION

Supernovae (SNe) are one of the most intriguing and least known phenomena in the universe. In this process, approximately 3×10^{53} erg of energy are emitted in form of neutrinos of all species in the energy range of MeV, which represent 99% of the total released energy (Lunardini 2006). Questions that are still open in neutrino physics such as their Dirac or Majorana nature (Barranco et al. 2020), their masses (Lu et al. 2015), the hierarchy between the masses (Serpico et al. 2012; Dighe & Smirnov 2000), and the neutrino magnetic moment (Ando & Sato 2003), are the motivation of current scientific research and could be solved by studying the high neutrino fluxes arriving to Earth from nearby SNe events. Current and future neutrino detectors, such as SNO+ (Albanese et al. 2021), Super-Kamiokande (Ikeda et al. 2007), KamLAND (Eguchi et al. 2003), HALO (Duba et al. 2008), JUNO (An et al. 2016), and Hyper-Kamiokande (Abe et al. 2018), are capable of detecting the neutrino flux coming from a supernova (SN) explosion in the Milky Way galaxy or the galactic neighborhood. Such neutrinos can also be detected on dark matter detectors through the process coherent elastic neutrino-nucleus scattering (CE ν NS) (Horowitz et al. 2003; Lang et al. 2016). This represents an invaluable opportunity for exploring neutrino properties and SN physics. On the other hand, there is a community of researchers dedicated to simulating the SN neutrino flux (Janka 2022), considering many parameters and variables. The EstrellaNueva software has been created to provide a link between the SN simulations and the expected observed signal in detectors. EstrellaNueva is a flexible and simple standalone tool that is valuable to promptly perform several studies when a SN takes place in the galaxy neighborhood.

The software package has several SN models implemented, the adiabatic Mikheyev–Smirnov–Wolfenstein (MSW) (Dighe & Smirnov 2000; Giunti & Wook 2007; Xu et al. 2014) effect for neutrino flavor transformation in the SN matter, and the analytical cross sections of the principal detection channels in current and future detectors. Another important and unique feature of this software is the option to design any target material. EstrellaNueva allows calculating the

fluences of the neutrinos coming from SNe, interaction rates, and total number of interactions with the target particles of the detectors. These characteristics are valuable for performing comparisons of events observed by detectors that are either currently operating or under design and construction.

In addition to EstrellaNueva, other software tools to study supernova neutrinos exist, but are generally not as simple to use and require additional software packages. For example, SNEWPY (Baxter et al. 2022) requires an event rate calculator or an event generator such as sntools (Migenda et al. 2021), while SNOwGLOBES (Scholberg et al. 2020) requires the GLOBES (Huber et al. 2005, 2007) software to perform the event rate calculations. EstrellaNueva provides all in a single package without requiring any other interface, and also provides an analytical implementation of the cross section functions and the option to input target materials with any chemical composition. This advantage makes possible the implementation of any SN model and any neutrino interaction in the detector. The modular implementation also makes it suitable to study other neutrino flavor scenarios, not only in the SN, but also when the neutrino propagates on Earth. The software currently considers flavor transformation via the adiabatic MSW effect in the SN.

In this manuscript, the EstrellaNueva software is presented with a description of the SN models used and the neutrino physics implemented, with some examples of its flexibility and simplicity. The followings sections are organized as follows: Section 2 shows the software structure; Section 3 describes a general overview of the implemented physics; Section 4 shows the implemented SN models; Section 5 presents the analytically implemented cross sections of the detection channels and the implemented nuclear form factors for the case of $CE\nu NS$ interaction; Section 6 shows two examples of the configuration file setup; finally Section 7 presents the conclusions.

2. SOFTWARE STRUCTURE

EstrellaNueva is open-source software written in Python designed to complement the supernova simulations, by calculating the interaction rates as well as the number of events in detectors. It was built using NumPy (Harris et al. 2020) and SciPy (Virtanen et al. 2020): two well-optimized Python modules that offer excellent tools to process large volumes of data and perform scientific calculations. It also uses the Python module Matplotlib (Hunter 2007) to plot the output functions as well as some of the implemented functions such as cross sections and nuclear form factors. The software is available in the Zenodo repository: <https://doi.org/10.5281/zenodo.6354850> (González-Reina & Vázquez-Jáuregui 2022).

The software package, stored in the directory “EstrellaNueva”, contains the following items:

- The main file “EstrellaNueva.py”: main script to execute the software. This Python script uses Python 3 as interpreter, from the directory “EstrellaNueva”. The command line for execution is: “python3 EstrellaNueva.py”.
- The configuration file “config.json”: JSON file for setting the configuration parameters, before executing the main script.
- The sub-directory “data”: contains the data of the supernova models, as well as some of the implemented cross sections which were taken from the SNOwGLOBES (Scholberg et al. 2020) repository in form of data files. These cross sections correspond to the interactions with ^{12}C , ^{16}O , and ^{208}Pb .
- The sub-directory “out”: will contain the output files once the code is executed. The output consists of data files with the number of interactions per channel, interaction rates, and fluences.
- The sub-directory “src”: contains the EstrellaNueva libraries. The cross sections implemented analytically are located in this directory.
- The sub-directory “doc”: contains the user manual.

The input requested by the code is:

- the supernova model,
- the neutrino mass ordering ¹

¹ The neutrino mass ordering is considered for the adiabatic MSW effect in the supernova matter. Flavor transformations can also be turned off.

- the distance to the supernova,
- the mass of the active volume of the detector and chemical composition of the material, and
- the detection channels;

and the output is:

- the interaction rates with respect to the incoming neutrino energy and time, in addition to the recoil particle energy, for the case of elastic scattering interactions,
- the fluences, and
- the total number of interactions.

3. FLAVOR TRANSFORMATION AND EXPECTED INTERACTION RATE

Most SN simulations report the time dependence of the neutrino flux at the neutrino-sphere. At this location inside the SN, it is assumed neutrinos can travel freely, without further diffusing with the SN matter due to their small interaction cross sections. The neutrino flux is assumed to be quasi-thermal in this sphere and can be parameterized by the following expression as a function of the neutrino energy E and the SN time t (the elapsed time taking the origin at the core bounce) (Keil et al. 2003; Serpico et al. 2012):

$$F_\nu^0(E, t) = \mathcal{L}_\nu(t) \frac{(1 + \beta_\nu(t))^{1 + \beta_\nu(t)}}{\Gamma(1 + \beta_\nu(t))} \frac{E^{\beta_\nu(t)}}{(\langle E_\nu \rangle(t))^{\beta_\nu(t) + 2}} \times \exp \left[-(\beta_\nu(t) + 1) \frac{E}{\langle E_\nu \rangle(t)} \right], \quad (1)$$

where \mathcal{L}_ν is the luminosity, $\langle E_\nu \rangle$ is the neutrino mean energy, β_ν is the so-called energy-shape parameter, and ν represents the neutrino states $\nu_e, \nu_\mu, \nu_\tau, \bar{\nu}_e, \bar{\nu}_\mu,$ and $\bar{\nu}_\tau$. The energy-shape parameter is given by

$$\beta_\nu(t) = \frac{2(\langle E_\nu \rangle(t))^2 - \langle E_\nu^2 \rangle(t)}{\langle E_\nu^2 \rangle(t) - (\langle E_\nu \rangle(t))^2}, \quad (2)$$

which quantifies how close the neutrino spectrum is to the black-body spectrum, as a function of time (Serpico et al. 2012). The primary fluxes at the neutrino-sphere F_ν^0 will be affected by neutrino flavor transformation on their path through the SN matter. One of the most common and accepted scenarios is the adiabatic MSW effect, which has been implemented in the EstrellaNueva framework.

3.1. Adiabatic MSW effect

An ultrarelativistic left-handed neutrino, born at the neutrino-sphere, with flavor α ($\alpha = e, \mu, \tau$) and momentum \vec{p} , is described by the flavor eigenstate

$$|\nu_\alpha\rangle = \sum_k U_{\alpha k}^* |\nu_k\rangle, \quad (3)$$

where U is the neutrino mixing matrix:

$$U = \begin{pmatrix} c_{12}c_{13} & s_{12}c_{13} & s_{13}e^{-i\delta} \\ -s_{12}c_{23} - c_{12}s_{23}s_{13}e^{i\delta} & c_{12}c_{23} - s_{12}s_{23}s_{13}e^{i\delta} & s_{23}c_{13} \\ s_{12}s_{23} - c_{12}s_{23}s_{13}e^{i\delta} & -c_{12}s_{23} - s_{12}c_{23}s_{13}e^{i\delta} & c_{23}c_{13} \end{pmatrix}, \quad (4)$$

with $s_{ij} = \sin \theta_{ij}$, $c_{ij} = \cos \theta_{ij}$. The θ_{ij} are mixing angles and δ is a Dirac CP² violating phase (de Salas et al. 2021). The symbol $|\nu_k\rangle$, where $k = 1, 2, 3$, represents an eigenstate of the vacuum Hamiltonian \mathcal{H}_0 :

$$\mathcal{H}_0 |\nu_k\rangle = E_k |\nu_k\rangle, \quad \text{with} \quad E_k = \sqrt{\vec{p}^2 + m_k^2}. \quad (5)$$

² CP is the combined charge conjugation (C) and parity (P) symmetry.

The total Hamiltonian in matter is

$$\mathcal{H} = \mathcal{H}_0 + \mathcal{H}_I, \quad \text{with} \quad \mathcal{H}_I|\nu_\alpha\rangle = V_\alpha|\nu_\alpha\rangle, \quad (6)$$

where V_α is the effective potential experienced by the ultrarelativistic left-handed flavor neutrino:

$$V_\alpha = V_{CC}\delta_{\alpha e} + V_{NC} = \sqrt{2}G_F \left(n_e\delta_{\alpha e} - \frac{1}{2}n_n \right). \quad (7)$$

In Equation (7), $\delta_{\alpha e}$ is the Kronecker delta, V_{CC} and V_{NC} are the effective potentials due to the charge current (CC) and neutral current (NC) interactions, and n_e and n_n are the electron and neutron density of the medium, respectively. In the Schrödinger picture, a neutrino state with initial flavor α obeys the evolution equation

$$i \frac{d}{dt} |\nu_\alpha(t)\rangle = \mathcal{H}|\nu_\alpha(t)\rangle, \quad \text{with} \quad |\nu_\alpha(0)\rangle = |\nu_\alpha\rangle. \quad (8)$$

For ultrarelativistic neutrinos the following approximation is valid:

$$E_k \simeq E + \frac{m_k^2}{2E}, \quad p \simeq E, \quad t \simeq x, \quad (9)$$

where x is the distance from the neutrino-sphere. Neglecting a common phase term, the evolution equation for the amplitude of the transition $\nu_\alpha \rightarrow \nu_\beta$, $\psi_{\alpha\beta} = \langle \nu_\beta | \nu_\alpha(t) \rangle$ (with $\beta = e, \mu, \tau$), can be written in matrix form as (Giunti & Wook 2007)

$$i \frac{d}{dx} \Psi_\alpha = \mathcal{H}_F \Psi_\alpha, \quad (10)$$

where \mathcal{H}_F is the effective Hamiltonian in the flavor basis:

$$\mathcal{H}_F = \frac{1}{2E} (U\mathbb{M}^2U^\dagger + \mathbb{A}). \quad (11)$$

In the case of three-neutrino mixing,

$$\Psi_\alpha = \begin{pmatrix} \psi_{\alpha e} \\ \psi_{\alpha \mu} \\ \psi_{\alpha \tau} \end{pmatrix}, \quad \mathbb{M}^2 = \begin{pmatrix} 0 & 0 & 0 \\ 0 & \Delta m_{21}^2 & 0 \\ 0 & 0 & \Delta m_{31}^2 \end{pmatrix}, \quad \mathbb{A} = \begin{pmatrix} A_{CC} & 0 & 0 \\ 0 & 0 & 0 \\ 0 & 0 & 0 \end{pmatrix}, \quad (12)$$

where Δm_{21}^2 and Δm_{31}^2 are the squared neutrino mass splittings, and

$$A_{CC}(x) \equiv 2EV_{CC}(x) = 2\sqrt{2}EG_F n_e(x). \quad (13)$$

An analogous mathematical development can be obtained for anti-neutrinos, where $A_{CC}(x) = -2\sqrt{2}EG_F n_e(x)$ due to the change in the sign of V_{CC} . More details about this description can be found in (Giunti & Wook 2007).

The primary fluxes coming from the neutrino-sphere are $F_{\nu_e}^0$, $F_{\bar{\nu}_e}^0$, and $F_{\nu_x}^0$, where $\nu_x = \nu_\mu, \nu_\tau, \bar{\nu}_\mu, \bar{\nu}_\tau$. Because non-electron type neutrinos have the same interactions inside the SN, their primary fluxes are expected to be approximately equal (Dighe & Smirnov 2000). It is useful to use the equality $F_{\nu_\mu}^0 = F_{\nu_\tau}^0 = F_{\nu_x}^0$ and perform a rotation in the $(|\nu_\mu\rangle, |\nu_\tau\rangle)$ plane changing the basis, $(|\nu_e\rangle, |\nu_\mu\rangle, |\nu_\tau\rangle) \rightarrow (|\nu_e\rangle, |\nu'_\mu\rangle, |\nu'_\tau\rangle)$:

$$|\nu'_\mu\rangle = \cos \theta_{23} |\nu_\mu\rangle - \sin \theta_{23} |\nu_\tau\rangle, \quad |\nu'_\tau\rangle = \sin \theta_{23} |\nu_\mu\rangle + \cos \theta_{23} |\nu_\tau\rangle, \quad (14)$$

as described in (Väänänen & Volpe 2011). This rotation ensures that $F_{\nu_x}^0 = F_{\nu'_\mu}^0 = F_{\nu'_\tau}^0$ and diagonalizes the (ν_μ, ν_τ) submatrix of \mathcal{H}_F :

$$\mathcal{H}_F^{rot} = \frac{1}{2E} \begin{pmatrix} m_{ee}^2 + A_{CC} & m_{e\mu'}^2 & m_{e\tau'}^2 \\ m_{e\mu'}^2 & m_{\mu'\mu'}^2 & 0 \\ m_{e\tau'}^2 & 0 & m_{\tau'\tau'}^2 \end{pmatrix}. \quad (15)$$

At high matter densities, close to the neutrino-sphere, the other off-diagonal elements of \mathcal{H}_F^{rot} can be neglected. This means that the flavor eigenstates $(|\nu_e\rangle, |\nu'_\mu\rangle, |\nu'_\tau\rangle)$ coincide with the effective matter eigenstates $(|\nu_{1m}\rangle, |\nu_{2m}\rangle, |\nu_{3m}\rangle)$

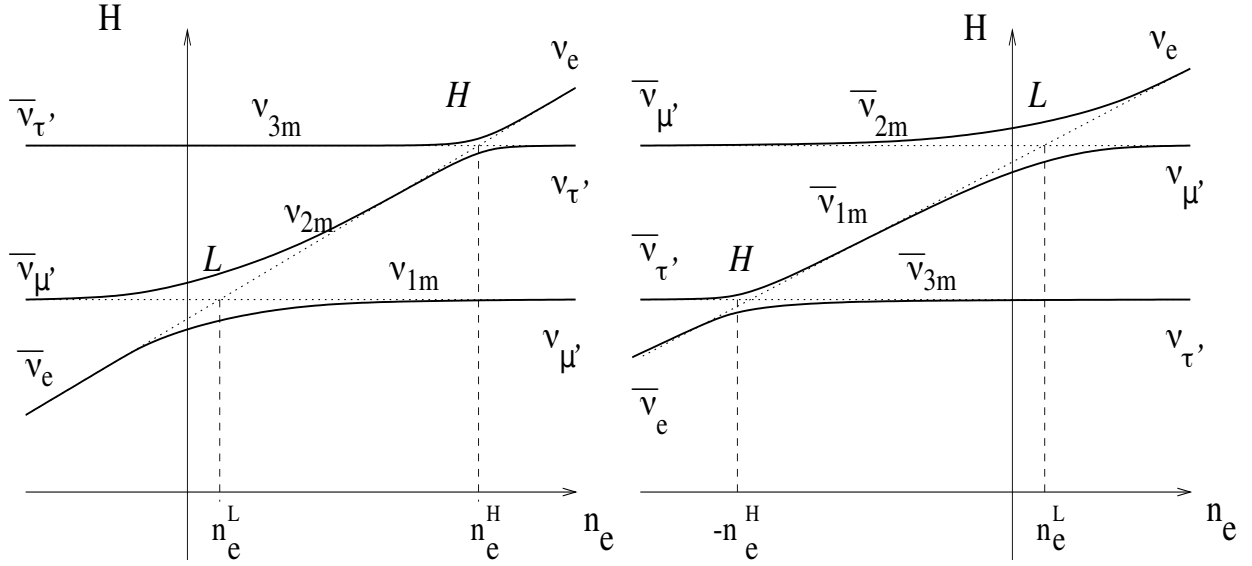


Figure 1. Level crossing diagrams for normal (left) and inverted (right) mass ordering of the neutrinos. Solid lines show the eigenvalues of the effective Hamiltonian \mathcal{H}_F^{rot} in the effective matter basis as function of the electron density n_e . Dashed lines correspond to energies of the flavor levels. The region with $n_e > 0$ refers to neutrinos, while the one with $n_e < 0$ to anti-neutrinos. L denotes the resonance region at low n_e and H the resonance region at high n_e . Figure reprinted with permission from (Dighe & Smirnov 2000) (<https://doi.org/10.1103/PhysRevD.62.033007>).

when they are produced. The rotated effective Hamiltonian \mathcal{H}_F^{rot} allows one to construct the level diagrams shown in Figure 1, for a given neutrino energy value (Dighe & Smirnov 2000). During the first second of the burst of neutrinos from a SN, in typical SN density profiles (model independent), the neutrino evolution can be considered adiabatically (Xu et al. 2014). This means that the transition probability between effective matter eigenstates can be neglected. Then, a neutrino born in an effective matter eigenstate will remain in this state during its path through the SN matter, until reaching the vacuum, where $|\nu_{km}\rangle \rightarrow |\nu_k\rangle$. Therefore, taking into account the mixing of the neutrinos and following the level diagrams shown in Figure 1, the neutrino fluxes in vacuum, considering the neutrino normal mass ordering (NO), can be written as a linear combination of the primary fluxes at the neutrino-sphere,

$$\begin{aligned}
F_{\nu_e} &= |U_{e1}|^2 F_{\nu_x}^0 + |U_{e2}|^2 F_{\nu_e}^0 + |U_{e3}|^2 F_{\nu_x}^0, \\
F_{\nu_\mu} &= |U_{\mu1}|^2 F_{\nu_x}^0 + |U_{\mu2}|^2 F_{\nu_e}^0 + |U_{\mu3}|^2 F_{\nu_x}^0, \\
F_{\nu_\tau} &= |U_{\tau1}|^2 F_{\nu_x}^0 + |U_{\tau2}|^2 F_{\nu_e}^0 + |U_{\tau3}|^2 F_{\nu_x}^0, \\
F_{\bar{\nu}_e} &= |U_{e1}|^2 F_{\bar{\nu}_e}^0 + |U_{e2}|^2 F_{\nu_x}^0 + |U_{e3}|^2 F_{\nu_x}^0, \\
F_{\bar{\nu}_\mu} &= |U_{\mu1}|^2 F_{\bar{\nu}_e}^0 + |U_{\mu2}|^2 F_{\nu_x}^0 + |U_{\mu3}|^2 F_{\nu_x}^0, \\
F_{\bar{\nu}_\tau} &= |U_{\tau1}|^2 F_{\bar{\nu}_e}^0 + |U_{\tau2}|^2 F_{\nu_x}^0 + |U_{\tau3}|^2 F_{\nu_x}^0.
\end{aligned} \tag{16}$$

Similarly, for the neutrino inverted mass ordering (IO) the neutrino fluxes in vacuum are

$$\begin{aligned}
F_{\nu_e} &= |U_{e1}|^2 F_{\nu_x}^0 + |U_{e2}|^2 F_{\nu_e}^0 + |U_{e3}|^2 F_{\nu_x}^0, \\
F_{\nu_\mu} &= |U_{\mu1}|^2 F_{\nu_x}^0 + |U_{\mu2}|^2 F_{\nu_e}^0 + |U_{\mu3}|^2 F_{\nu_x}^0, \\
F_{\nu_\tau} &= |U_{\tau1}|^2 F_{\nu_x}^0 + |U_{\tau2}|^2 F_{\nu_e}^0 + |U_{\tau3}|^2 F_{\nu_x}^0, \\
F_{\bar{\nu}_e} &= |U_{e1}|^2 F_{\nu_x}^0 + |U_{e2}|^2 F_{\nu_x}^0 + |U_{e3}|^2 F_{\bar{\nu}_e}^0, \\
F_{\bar{\nu}_\mu} &= |U_{\mu1}|^2 F_{\nu_x}^0 + |U_{\mu2}|^2 F_{\nu_x}^0 + |U_{\mu3}|^2 F_{\bar{\nu}_e}^0, \\
F_{\bar{\nu}_\tau} &= |U_{\tau1}|^2 F_{\nu_x}^0 + |U_{\tau2}|^2 F_{\nu_x}^0 + |U_{\tau3}|^2 F_{\bar{\nu}_e}^0.
\end{aligned} \tag{17}$$

3.2. Interaction rates

The neutrino interaction rates in a detector on Earth are determined for the flavour fluxes F_ν emitted by the SN as given in Equations (16) and (17). The number of interactions per unit time and energy is

$$\frac{d^2 N_\nu}{dE dt}(E, t) = \frac{N_t}{4\pi d^2} \sigma_\nu(E) F_\nu(E, t), \quad (18)$$

where d is the distance to the SN, N_t the number of target particles in the active volume of the detector, and σ_ν is the total cross section as a function of the incoming neutrino energy for a given interaction channel. Here is useful to define a magnitude so-called fluence, which is the time-integrated flux at Earth and provides the energy spectrum of the incoming neutrinos:

$$\lambda_\nu(E) = \frac{1}{4\pi d^2} \int_{t_0}^{t_{end}} F_\nu(E, t) dt. \quad (19)$$

In Equation (19), $(t_0; t_{end})$ is the time interval of the SN process. Integrating Equation (18), the interaction rates with respect to E and t are

$$\frac{dN_\nu}{dE}(E) = \int_{t_0}^{t_{end}} dt \left[\frac{d^2 N_\nu}{dE dt}(E, t) \right] = N_t \sigma_\nu(E) \lambda_\nu(E), \quad (20)$$

and

$$\frac{dN_\nu}{dt}(t) = \int_0^\infty dE \left[\frac{d^2 N_\nu}{dE dt}(E, t) \right], \quad (21)$$

respectively.

In the case of elastic scattering interactions, like neutrino-electron ($\nu - e$) elastic scattering, neutrino-proton ($\nu - p$) elastic scattering, and CE ν NS, it is possible to calculate the event rates with respect to the recoil particle energy T . The number of interactions per unit time, unit energy, and unit recoil energy is given by

$$\frac{d^3 N_\nu}{dE dT dt}(E, T, t) = \frac{N_t}{4\pi d^2} \frac{d\sigma_\nu}{dT}(E, T) F_\nu(E, t), \quad (22)$$

where $\frac{d\sigma_\nu}{dT}$ is the differential cross section with respect to T , which is related to the total cross section as follows:

$$\sigma_\nu(E) = \int_0^{T_{max}(E)} \frac{d\sigma_\nu}{dT}(E, T) dT, \quad (23)$$

where

$$T_{max}(E) = \frac{2E^2}{2E + m}, \quad (24)$$

is the maximum energy of the recoil particle, and m its mass. From Equation (22), the interaction rate with respect to T is obtained as follows,

$$\frac{dN_\nu}{dT}(T) = \int_{t_0}^{t_{end}} dt \int_{E_{min}(T)}^\infty dE \left[\frac{d^3 N_\nu}{dE dT dt}(E, T, t) \right] = N_t \int_{E_{min}(T)}^\infty dE \left[\frac{d\sigma_\nu}{dT}(E, T) \lambda_\nu(E) \right], \quad (25)$$

where

$$E_{min}(T) = \frac{T + \sqrt{T(T + 2m)}}{2}, \quad (26)$$

is the minimum energy required by the incoming neutrino. Finally, the total number of interactions is

$$N_\nu = \int_0^\infty dE \left[\frac{dN_\nu}{dE}(E) \right] = \int_{t_0}^{t_{end}} dt \left[\frac{dN_\nu}{dt}(t) \right] = \int_0^\infty dT \left[\frac{dN_\nu}{dT}(T) \right]. \quad (27)$$

4. SUPERNOVA MODELS

The EstrellaNueva software was specifically developed for complementing the simulations made by various supernova simulation groups in estimating the interaction rates expected in detectors. Currently, there are implemented several supernova models in the software package. The models are the result of simulations performed by the Core-Collapse Modeling Group at the Max Planck Institute for Astrophysics (Janka 2022), that reports the time dependence of the

Model	Progenitor Mass [M_{\odot}]	EoS	Time interval [s]	Reference
LS220-s11.2	11.2	LS220	-0.170092974551 – 0.500004733154	(Janka 2022)
LS220-s11.2c	11.2	LS220	-0.170092974551 – 7.600478503686	(Mirizzi et al. 2016; Janka 2022)
LS220-s12.0	12.0	LS220	-0.187296800690 – 0.497543448537	(Janka 2022)
LS220-s15.0	15.0	LS220	-0.304032523673 – 0.498446483650	(Janka 2022)
LS220-s15s7b2	15.0	LS220	-0.221282374565 – 0.496251020000	(Janka 2022)
LS220-s17.6	17.6	LS220	-0.284925820013 – 0.498178366419	(Janka 2022)
LS220-s17.8	17.8	LS220	-0.279131376354 – 0.500068432690	(Janka 2022)
LS220-s20.0	20.0	LS220	-0.256519704513 – 0.499980285627	(Janka 2022)
LS220-s20.6	20.6	LS220	-0.412889509135 – 0.500009131565	(Janka 2022)
LS220-s25.0	25.0	LS220	-0.455379448410 – 0.499728493980	(Janka 2022)
LS220-s27.0	27.0	LS220	-0.344627618270 – 0.497878869527	(Janka 2022)
LS220-s27.0c	27.0	LS220	-0.344627618270 – 8.350202515285	(Mirizzi et al. 2016; Janka 2022)
LS220-s27.0co	27.0	LS220	-0.349455361517 – 15.439433579436	(Mirizzi et al. 2016; Janka 2022)
LS220-z9.6co	9.6	LS220	-0.233381022196 – 11.999932339246	(Mirizzi et al. 2016; Janka 2022)
LS220-s40.0c	40.0	LS220	-0.408731709799 – 2.105601215751	(Mirizzi et al. 2016; Janka 2022)
LS220-s40s7b2c	40.0	LS220	-0.408737176878 – 0.567932280255	(Mirizzi et al. 2016; Janka 2022)
SFHo-s27.0co	27.0	SFHo	-0.292910194783 – 11.169139356183	(Janka 2022)
SFHo-z9.6co	9.6	SFHo	-0.242266894100 – 13.622987243331	(Mirizzi et al. 2016; Janka 2022)
Shen-s8.8	8.8	Shen	-0.0636472236 – 8.90975001	(Hüdepohl et al. 2010; Janka 2022)
Shen-s11.2	11.2	Shen	-0.136560972782 – 0.495312224658	(Janka 2022)
Shen-s12.0	12.0	Shen	-0.144379115573 – 0.495545475007	(Janka 2022)
Shen-s15.0	15.0	Shen	-0.211057570069 – 0.499739838584	(Janka 2022)
Shen-s15s7b2	15.0	Shen	-0.167861670324 – 0.500369261592	(Janka 2022)
Shen-s17.6	17.6	Shen	-0.199208094334 – 0.498790872514	(Janka 2022)
Shen-s17.8	17.8	Shen	-0.190373490538 – 0.498689914046	(Janka 2022)
Shen-s20.0	20.0	Shen	-0.187767329639 – 0.500071977502	(Janka 2022)
Shen-s20.6	20.6	Shen	-0.254702334699 – 0.499291328668	(Janka 2022)
Shen-s25.0	25.0	Shen	-0.275634063374 – 0.496790109348	(Janka 2022)
Shen-s27.0	27.0	Shen	-0.227437666075 – 0.496242346477	(Janka 2022)
Shen-s40.0	40.0	Shen	-0.254058543569 – 0.500396111047	(Janka 2022)

Table 1. Supernova models from the Core-Collapse Modeling Group at the Max Planck Institute for Astrophysics (Janka 2022), available in the software EstrellaNueva.

primary flux parameters at the neutrino-sphere, namely $\mathcal{L}_{\nu}(t)$, $\langle E_{\nu} \rangle(t)$, and $\langle E_{\nu}^2 \rangle(t)$. The time dependence of β_{ν} is calculated by EstrellaNueva following Equation (2). These models were simulated with the PROMETEUS-VERTEX code (Müller et al. 2010; Serpico et al. 2012) using three different equations of state: the equation of state (EoS) of Lattimer and Swesty (Lattimer & Douglas Swesty 1991), with a nuclear incompressibility of 220 MeV, denoted by LS220; the Shen EoS (Shen et al. 1998); and the SFHo hadronic EoS (Steiner et al. 2013). Implemented SN models are described in Table 1, where the time intervals in which they were simulated are also shown. As an example, Figure 2 shows the time dependence of the primary flux parameters for the model LS220-s15.0, which corresponds to a progenitor of mass 15.0 M_{\odot} (M_{\odot} is the mass of the Sun) and was simulated using the LS220 EoS. Figure 3 shows the fluences for this model at a distance to the SN equal to 10 kpc, considering the MSW effect with NO, IO, and neglecting the neutrino flavor transformation in the SN matter. For fluence calculations, the entire time interval of the model was used.

In addition, it is possible to define a simple and time-independent SN model in the EstrellaNueva software. This is assuming the primary flux parameters constant in time. In this scenario, the fluences of the primary fluxes are given

by the following expression:

$$\begin{aligned} \lambda_\nu^0 &= \frac{1}{4\pi d^2} \int_{t_0}^{t_{end}} F_\nu^0(E, t) dt \\ &= \frac{\varepsilon_\nu}{4\pi d^2} \frac{(1 + \beta_\nu)^{1+\beta_\nu}}{\Gamma(1 + \beta_\nu)} \frac{E^{\beta_\nu}}{(\langle E_\nu \rangle)^{\beta_\nu+2}} \times \exp \left[-(\beta_\nu + 1) \frac{E}{\langle E_\nu \rangle} \right], \end{aligned} \quad (28)$$

where ε_ν is the total energy emitted from the neutrino-sphere in form of neutrinos of the specie ν . Then, if the adiabatic MSW effect is considered, the flavor transformed fluences λ_ν are linear combinations of the primary fluences λ_ν^0 , which are calculated following Equations (16) or (17) depending on the neutrino mass ordering assumed. The primary fluxes F_ν^0 are replaced by the primary fluences λ_ν^0 for this case. The values of the parameters ε_ν , $\langle E_\nu \rangle$, and β_ν are requested as input for the neutrino species considered in the neutrino-sphere.

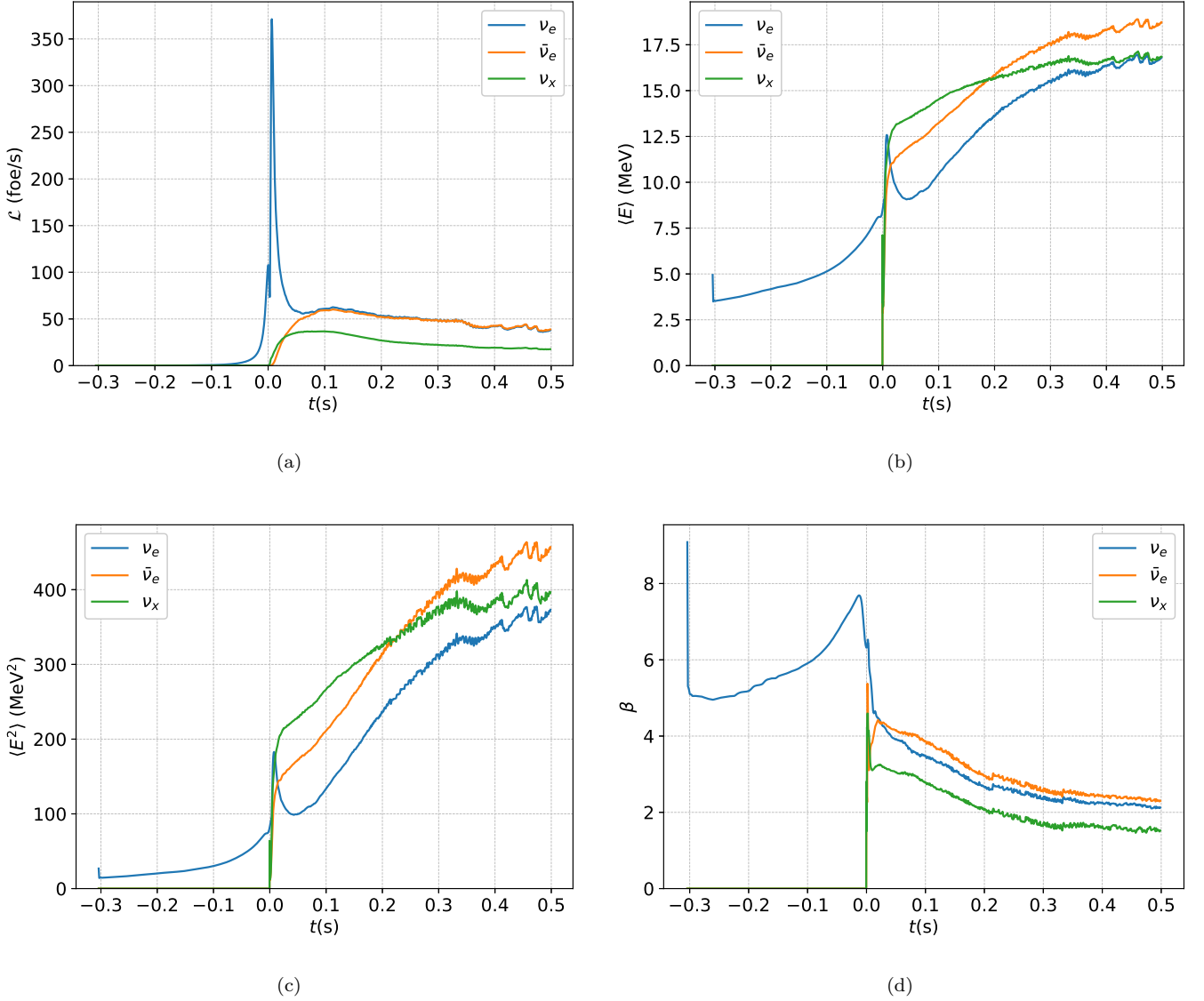
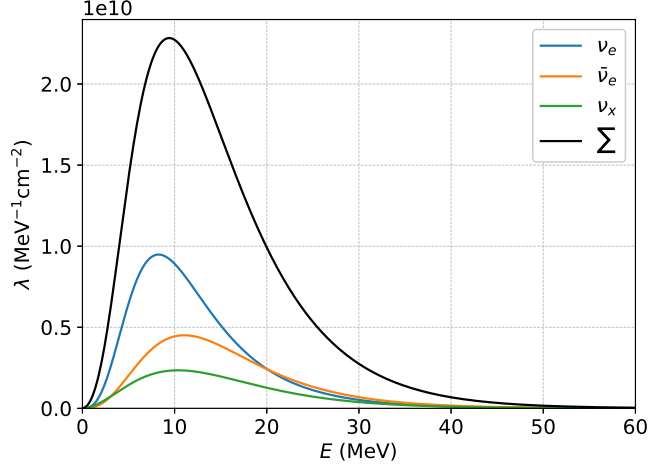
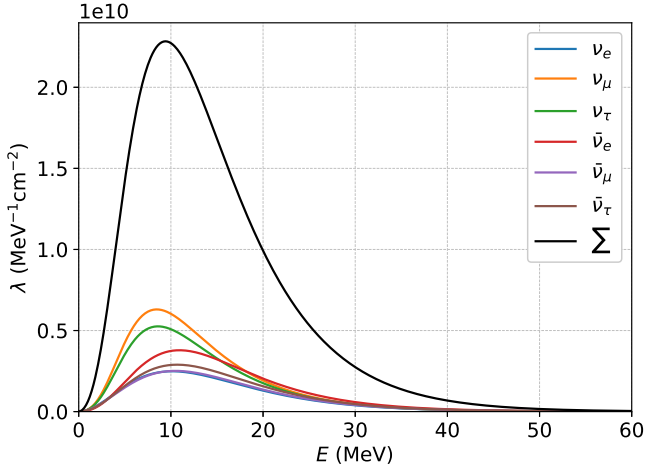


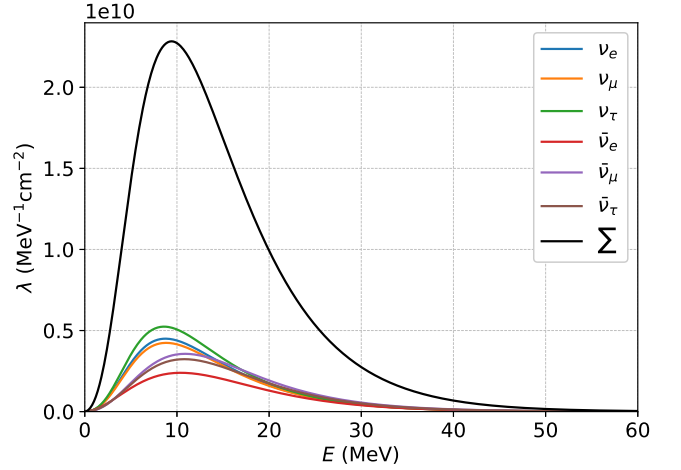
Figure 2. Time dependence of the primary flux parameters corresponding to the SN model LS220-s15.0 (Janka 2022). (a) Luminosity, (b) mean energy, (c) mean squared energy, and (d) energy-shape parameter, which was calculated following Equation (2).



(a)



(b)



(c)

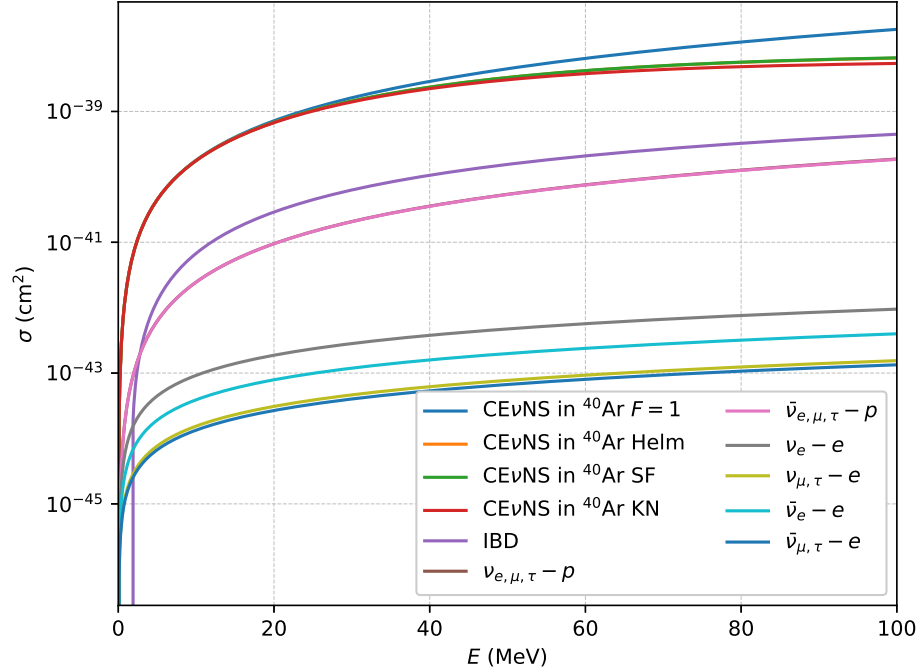
Figure 3. Fluences corresponding to the SN model LS220-s15.0 (Janka 2022), assuming a distance to the SN equal to 10 kpc, considering (a) no neutrino flavor transformation in the SN matter and the adiabatic MSW effect with (b) NO and (c) IO. The full SN simulation time interval is considered. In the case of NO, fluences corresponding to ν_e and $\bar{\nu}_\mu$ are superimposed.

5. DETECTION CHANNELS

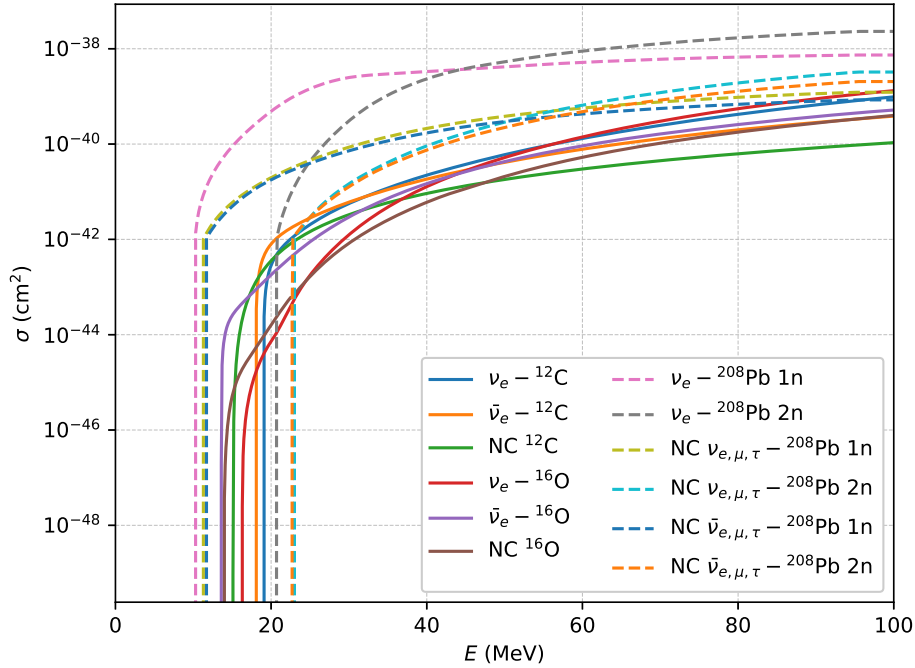
EstrellaNueva has implemented the cross sections of the principal detection channels for materials employed by current and future detectors, such as water, argon, xenon, lead, and mineral liquid scintillators. In addition, the software provides the flexibility to define materials with any chemical composition. The detection channels implemented are: $\nu - e$ elastic scattering, $\nu - p$ elastic-scattering, inverse beta decay (IBD), coherent elastic neutrino-nucleus scattering (CE ν NS), and the interactions with ^{12}C , ^{16}O , and ^{208}Pb . The last three were taken from the SNOwGLoBES repository (Scholberg et al. 2020) in the form of data files and the rest were implemented analytically. The implementation of analytical cross sections is one of the main features provided by this software package.

The analytical expression for the $\nu - e$ elastic scattering differential cross section, taken from (Giunti & Studenikin 2015), is

$$\frac{d\sigma_\nu}{dT}(E, T) = \frac{G_F^2 m_e}{2\pi} \left\{ (g_V^\nu + g_A^\nu)^2 + (g_V^\nu - g_A^\nu)^2 \left(1 - \frac{T}{E}\right)^2 + [(g_A^\nu)^2 - (g_V^\nu)^2] \frac{m_e T}{E^2} \right\}, \quad (29)$$



(a)



(b)

Figure 4. Cross sections as function of the incoming neutrino energy E . (a) In the case of scattering interactions with protons, the cross sections for neutrinos and antineutrinos are superimposed. The cross sections for CE ν NS in ^{40}Ar corresponding to the Helm and SF form factors are also superimposed. $F = 1$ assumes a form factor equal to one. (b) NC are neutral current interactions, while the rest are charge current interactions. In the case of interactions with ^{208}Pb , (1n) and (2n) result in one and two neutrons, respectively. See (Scholberg et al. 2020) for references.

where m_e is the electron mass and G_F the Fermi coupling constant. The coupling constants g_V^ν and g_A^ν are related to the effective weak mixing angle θ_W ($\sin^2 \theta_W = 0.23153$ (Tiesinga et al. 2021)) as follows,

$$g_V^{\nu e} = 2 \sin^2 \theta_W + 1/2, \quad g_A^{\nu e} = 1/2, \quad (30)$$

$$g_V^{\nu \mu, \tau} = 2 \sin^2 \theta_W - 1/2, \quad g_A^{\nu \mu, \tau} = -1/2, \quad (31)$$

$$g_V^{\bar{\nu} e} = 2 \sin^2 \theta_W + 1/2, \quad g_A^{\bar{\nu} e} = -1/2, \quad (32)$$

$$g_V^{\bar{\nu} \mu, \tau} = 2 \sin^2 \theta_W - 1/2, \quad g_A^{\bar{\nu} \mu, \tau} = 1/2. \quad (33)$$

For $\nu - p$ elastic scattering, the differential cross section, taken from (Beacom et al. 2002), is given by

$$\frac{d\sigma_\nu}{dT}(E, T) = \frac{G_F^2 m_p}{2\pi E^2} \left[(c_V \pm c_A)^2 E^2 + (c_V \mp c_A)^2 (E - T)^2 - (c_V^2 - c_A^2) m_p T \right], \quad (34)$$

where m_p represents the proton mass. c_A and c_V are the axial-vector and vector coupling constants between the exchanged Z^0 boson and the proton, with

$$c_V = \frac{1 - 4 \sin^2 \theta_W}{2} \quad \text{and} \quad c_A = \frac{g_A(0) \cdot (1 + \eta)}{2}, \quad (35)$$

where $g_A(0) = 1.267$ is the axial proton form factor (Beringer et al. 2012) and $\eta = 0.12$ is the proton strangeness (Ahrens et al. 1987). The upper sign refers to neutrinos and the lower to anti-neutrinos.

For the IBD interaction a simple but accurate approximation for SN neutrino energies ($E < 300$ MeV) is implemented. The total cross section as a function of the incoming $\bar{\nu}_e$ energy is given by (Strumia & Vissani 2003)

$$\sigma_{\text{IBD}}(E) = 10^{-43} \text{cm}^2 p_{e^+} E_{e^+}^{\text{tot}} E^{-0.07056 + 0.02018 \ln E - 0.001953 \ln^3 E}, \quad (36)$$

where $E_{e^+}^{\text{tot}} \approx E - (m_n - m_p)$, with m_n representing the neutron mass; and p_{e^+} is the positron momentum. This interaction has a threshold energy given by

$$E_{\text{thr}} = \frac{(m_n + m_e)^2 - m_p^2}{2m_p} \approx 1.806 \text{ MeV}. \quad (37)$$

Lastly, in the case of CE ν NS, the differential cross section is taken from (Liao et al. 2021) and given by the following expression,

$$\frac{d\sigma}{dT}(E, T) = \frac{G_F^2 M}{4\pi} q_W^2 \left(1 - \frac{MT}{E^2} \right) F^2(q^2), \quad (38)$$

where M is the target nucleus mass, $q_W = N - (1 - 4 \sin^2 \theta_W) Z$ is the weak nuclear charge with N and Z the number of neutrons and protons in the target nucleus, respectively. $F(q^2)$ is the nuclear form factor as function of the transferred momentum q . The following nuclear form factors are implemented: the Helm form factor, the symmetrized Fermi (SF) form factor, and the Klein-Nystrand (KN) form factor. A nuclear form factor equal to one can also be assumed. Next, the analytical expressions of the nuclear form factors will be discussed.

The analytical expression for the Helm form factor parameterization is given by (Lewin & Smith 1996; Papoulias et al. 2020)

$$F_{\text{Helm}}(q^2) = 3 \frac{j_1(qR_0)}{qR_0} e^{-(qs)^2/2}, \quad (39)$$

where j_1 denotes the 1st-order spherical Bessel function, $s = 0.9$ fm is the nuclear surface thickness, and $R_0 = \sqrt{c^2 + \frac{7}{3}\pi^2 a^2 + s^2}$ is the effective nuclear radius, the so-called diffraction radius. $c = 1.23A^{1/3} - 0.60$ fm and $a = 0.52$ fm represent the half density radius and the diffuseness, respectively, where A is the mass number of the target nucleus.

The analytical expression for the SF form factor is given by (Papoulias et al. 2020)

$$F_{\text{SF}}(q^2) = \frac{3}{qc [(qc)^2 + (\pi qa)^2]} \left[\frac{\pi qa}{\sinh(\pi qa)} \right] \left[\frac{\pi qa \sin(qc)}{\tanh(\pi qa)} - qc \cos(qc) \right]. \quad (40)$$

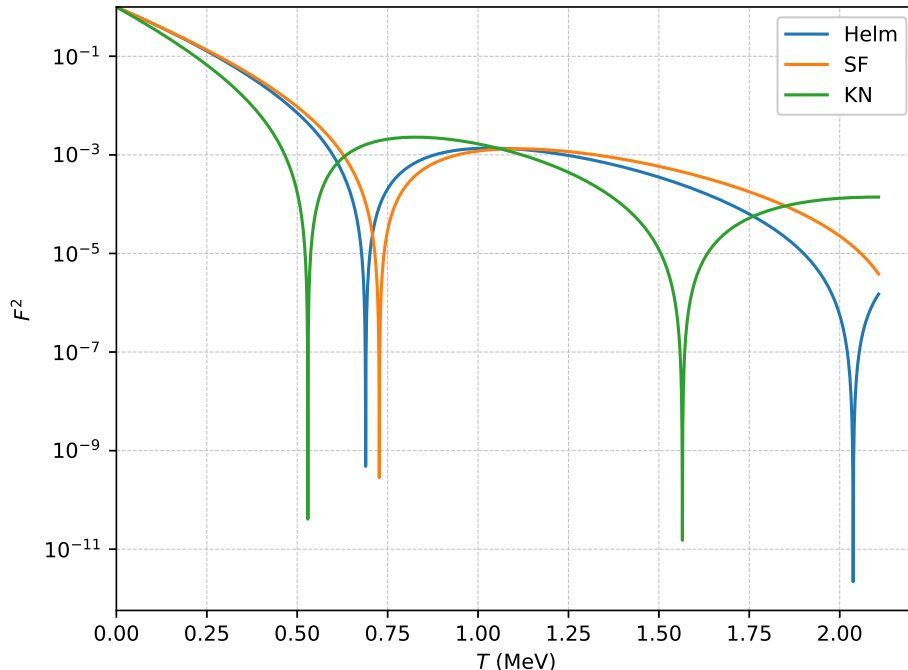


Figure 5. Nuclear form factors for ^{40}Ar as function of the nucleus recoil energy T .

Finally, in the case of the KN form factor, the implemented analytical expression is given by (Papoulias et al. 2020; Liao et al. 2021)

$$F_{\text{KN}} = \frac{4\pi\rho_0}{Aq^3} (\sin(qR_A) - qR_A \cos(qR_A)) \frac{1}{1 + (qa_k)^2}, \quad (41)$$

where $a_k = 0.7$ fm is the range of a Yukawa potential which is convoluted over a Woods-Saxon distribution, approximated as a hard sphere with radius $R_A = A^{1/3}r_0$, with the proton radius $r_0 = 1.3$ fm, and $\rho_0 = \frac{3}{4\pi r_0^3}$ is the nuclear density. $q^2 \approx 2MT$ is considered to evaluate the nuclear form factors as functions of the recoil nucleus energy.

Figure 4 shows the cross sections implemented in EstrellaNueva, with the cross section for $\text{CE}\nu\text{NS}$ in ^{40}Ar (as an example) using the form factors considered in the software. Figure 5 shows the Helm, SF, and KN form factors for ^{40}Ar .

6. CONFIGURATION FILE EXAMPLES FOR ESTRELLANUEVA

The EstrellaNueva software is a standalone code that does not require any more dependencies other than the Python modules that were used for its programming. The modules are Numpy (Harris et al. 2020), Scipy (Virtanen et al. 2020), and Mathplotlib (Hunter 2007). These modules are required in the Python3 environment.

In this section, two examples of the configuration file are presented to calculate interaction rates. The SN model LS220-s15.0, presented in Sec. 4, is used as example, with the distance to the SN assumed at 10 kpc and considering the full SN simulation time interval. The fluences regarding this configuration for the neutrino flavor transformation scenarios implemented (adiabatic MSW effect with normal and inverted neutrino mass ordering, and no neutrino flavor transformation) are shown in Figure 3.

6.1. Interaction rates for $\nu - e$ elastic scattering in a 100 kton detector using liquid scintillator

In this example, the interaction rates for $\nu - e$ elastic scattering are calculated for a 100 kton generic detector with linear alkylbenzene (LAB). LAB is used as a target medium by the SNO+ experiment (Albanese et al. 2021) and it will be used by the future JUNO experiment (Cao et al. 2019). LAB is a material internally predefined in the software, although any chemical composition can be defined in the configuration file. The configuration to compute the interaction rates, considering normal neutrino mass ordering (NO), is as follows,

```
{
"model": "ls220_s15.0",
"msw": "NO",
"distance": 10,
"material": "LAB",
"detector_mass": 100,
"interactions": ["nue_e", "numu_e", "nutau_e", "nuebar_e", "numubar_e", "nutaubar_e"]
}
```

Figure 6 shows the interaction rates obtained from the above configuration. The total number of events for each channel are shown in Table 2.

Channel	Events
$\nu_e - e$	212.21
$\nu_\mu - e$	59.94
$\nu_\tau - e$	53.30
$\bar{\nu}_e - e$	135.64
$\bar{\nu}_\mu - e$	31.53
$\bar{\nu}_\tau - e$	35.93
Total	528.55

Table 2. Number of interactions for $\nu - e$ elastic scattering in 100 kton of LAB, in the NO scenario for the MSW flavor transformation, and assuming model LS220-s15.0 at a distance of 10 kpc. The full SN simulation time interval is considered.

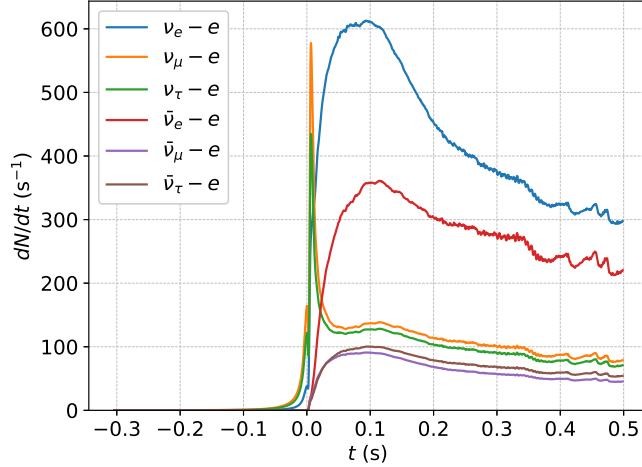
6.2. Interaction rates for $CE\nu NS$ in a 100 tonne detector using liquid argon

Nuclear form factor	Events
$F = 1$	279.13
Helm	255.11
SF	255.17
KN	249.34

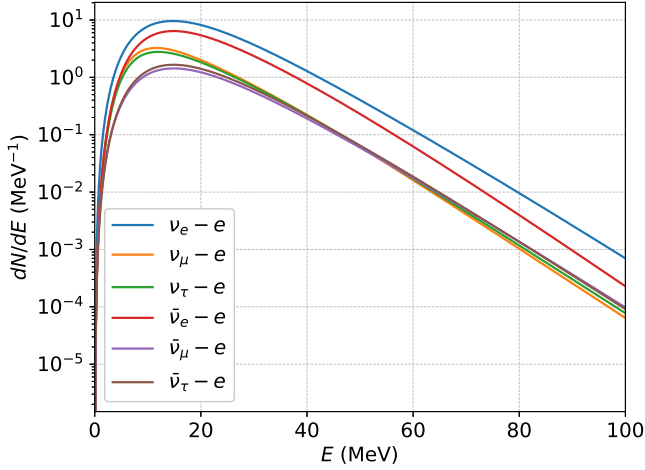
Table 3. Number of interactions for $CE\nu NS$ in 100 tonnes of ^{40}Ar for the form factors considered. The SN model LS220-s15.0 is used assuming a distance to the SN of 10 kpc and considering no neutrino flavor transformation in the SN matter. The full SN simulation time interval is considered.

This example corresponds to the event rates calculated for $CE\nu NS$ in 100 tonnes of liquid argon, considering a chemical composition of pure ^{40}Ar . Argon is also predefined internally. $CE\nu NS$ interactions are not affected by flavor transformations and they are turned off in this case. The results do not change if flavor transformations are included. The configuration file for the implemented nuclear form factors is as follows:

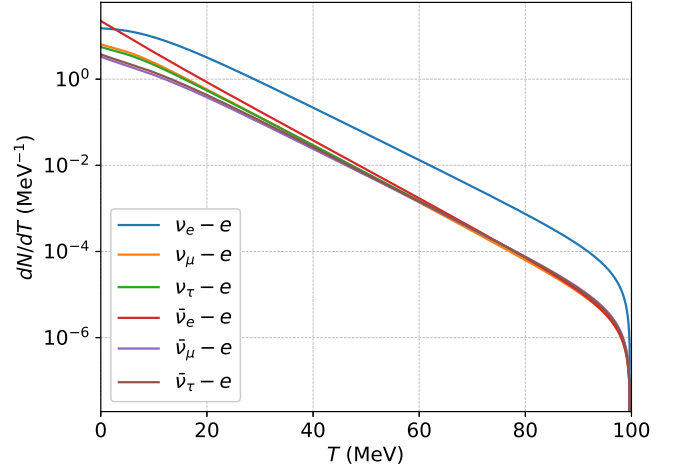
```
{
"model": "ls220_s15.0",
"msw": "off",
"distance": 10,
"material": "Argon",
"detector_mass": 0.1,
"interactions": ["CEnuNS_Ar40_one", "CEnuNS_Ar40_Helm", "CEnuNS_Ar40_Symmetrized_Fermi",
"CEnuNS_Ar40_Klein_Nystrand"]
}
```



(a)



(b)



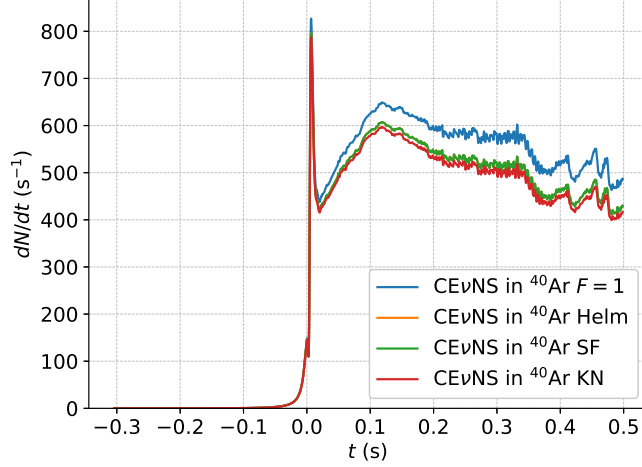
(c)

Figure 6. Interaction rates with respect to (a) time t , (b) incoming neutrino energy E , and (c) recoil electron energy T for $\nu - e$ elastic scattering in 100 kton of LAB. The NO scenario for the adiabatic MSW flavor transformation is assumed and model LS220-s15.0 is used at a distance of 10 kpc. The full SN simulation time interval is considered.

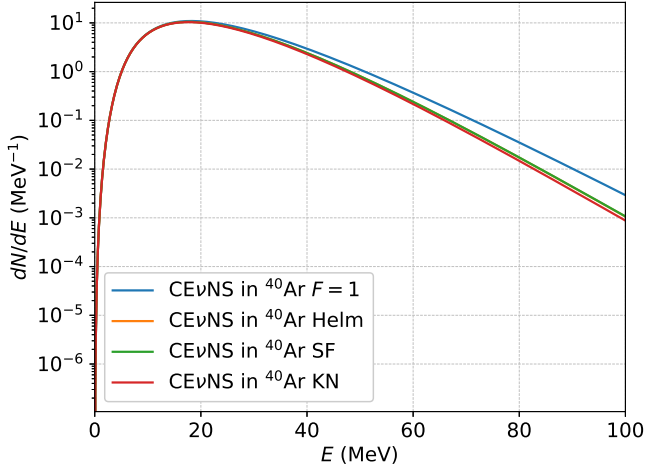
The interaction rates obtained from the above configuration file are shown in Figure 7. Table 3 shows the number of interactions for each nuclear form factor. A complete and detailed guide of the EstrellaNueva software is included in the Zenodo repository.

7. CONCLUSIONS

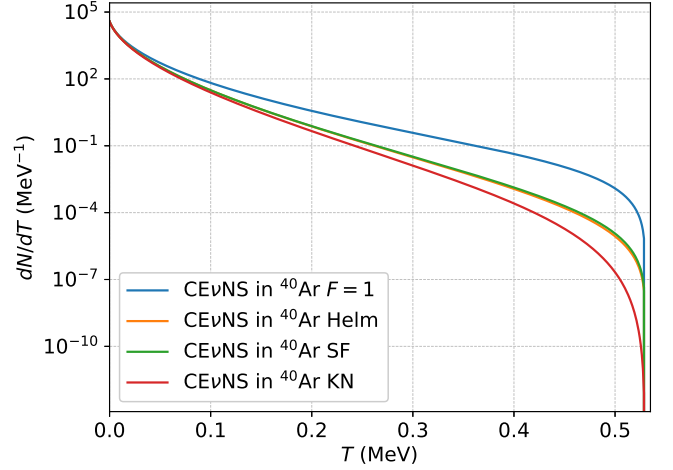
Several detectors all over the world are currently expecting the emergence of a supernova. Thousands of events are expected in current operating neutrino detectors. Simple, flexible, standalone, and independent tools are valuable and will be useful when such a cosmic event takes place. The EstrellaNueva software provides a user-friendly tool to study neutrinos and supernova properties by calculating the number of events in detectors. Several detection channels are currently implemented, the majority with analytical functions, such as neutrino-electron and neutrino-proton elastic scattering, inverse beta decay, and coherent elastic neutrino-nucleus scattering with the Helm, Klein-Nystrand, and symmetrized Fermi nuclear form factors. The adiabatic MSW effect for the neutrino flavor transformations in the supernova matter is also implemented. EstrellaNueva considers several supernova models simulated by the Core-



(a)



(b)



(c)

Figure 7. Interaction rates for CE ν NS in 100 tonnes of ^{40}Ar . The SN model LS220-s15.0 is used assuming a distance to the SN of 10 kpc and considering no neutrino flavor transformation in the SN matter. The full SN simulation time interval is considered. The interaction rates for the Helm and the SF nuclear form factors are superimposed. Rates are shown with respect to (a) time t , (b) incoming neutrino energy E , and (c) recoil nucleus energy T .

Collapse Modeling Group at the Max Planck Institute for Astrophysics. In addition, the primary flux parameters can be considered constant in time, which is useful to study soft regions of the supernova neutrino spectrum. This software complements other tools available to the supernova physics community, with the surplus of its simplicity and flexibility.

ACKNOWLEDGEMENTS

The authors would like to thank Hans-Thomas Janka and the Core-Collapse Modeling Group at the Max Planck Institute for Astrophysics, for granting access to their database. The authors also thank Eduardo Peinado and Leon M. G. de la Vega from IF-UNAM and the Supernova group of the SNO+ collaboration, for useful discussions.

This work is supported by the projects CONACYT CB-2017-2018/A1-S-8960, DGAPA UNAM grant PAPIIT-IN108020, and Fundación Marcos Moshinsky.

REFERENCES

- Abe, K., et al. 2018. <https://arxiv.org/abs/1805.04163>
- Ahrens, L. A., Aronson, S. H., Connolly, P. L., et al. 1987, *Phys. Rev. D*, 35, 785, doi: [10.1103/PhysRevD.35.785](https://doi.org/10.1103/PhysRevD.35.785)
- Albanese, V., Alves, R., Anderson, M., et al. 2021, *Journal of Instrumentation*, 16, P08059, doi: [10.1088/1748-0221/16/08/p08059](https://doi.org/10.1088/1748-0221/16/08/p08059)
- An, F., An, G., An, Q., et al. 2016, *Journal of Physics G: Nuclear and Particle Physics*, 43, 030401, doi: [10.1088/0954-3899/43/3/030401](https://doi.org/10.1088/0954-3899/43/3/030401)
- Ando, S., & Sato, K. 2003, *Phys. Rev. D*, 67, 023004, doi: [10.1103/PhysRevD.67.023004](https://doi.org/10.1103/PhysRevD.67.023004)
- Barranco, J., Delepine, D., Napsuciale, M., & Yebra, A. 2020, *Journal of Physics G: Nuclear and Particle Physics*, 47, 035201, doi: [10.1088/1361-6471/ab5079](https://doi.org/10.1088/1361-6471/ab5079)
- Baxter, A. L., BenZvi, S., Jaimes, J. C., et al. 2022, *The Astrophysical Journal*, 925, 107, doi: [10.3847/1538-4357/ac350f](https://doi.org/10.3847/1538-4357/ac350f)
- Beacom, J. F., Farr, W. M., & Vogel, P. 2002, *Phys. Rev. D*, 66, 033001, doi: [10.1103/PhysRevD.66.033001](https://doi.org/10.1103/PhysRevD.66.033001)
- Beringer, J., Arguin, J. F., Barnett, R. M., et al. 2012, *Phys. Rev. D*, 86, 010001, doi: [10.1103/PhysRevD.86.010001](https://doi.org/10.1103/PhysRevD.86.010001)
- Cao, D., Zhang, R., Liu, Y., et al. 2019, *Nuclear Instruments and Methods in Physics Research Section A: Accelerators, Spectrometers, Detectors and Associated Equipment*, 927, 230, doi: <https://doi.org/10.1016/j.nima.2019.01.077>
- de Salas, P. F., Forero, D. V., Gariazzo, S., et al. 2021, *JHEP*, 02, 071, doi: [10.1007/JHEP02\(2021\)071](https://doi.org/10.1007/JHEP02(2021)071)
- Dighe, A. S., & Smirnov, A. Y. 2000, *Phys. Rev. D*, 62, 033007, doi: [10.1103/PhysRevD.62.033007](https://doi.org/10.1103/PhysRevD.62.033007)
- Duba, C. A., Duncan, F., Farine, J., et al. 2008, *Journal of Physics: Conference Series*, 136, 042077, doi: [10.1088/1742-6596/136/4/042077](https://doi.org/10.1088/1742-6596/136/4/042077)
- Eguchi, K., Enomoto, S., Furuno, K., et al. 2003, *Phys. Rev. Lett.*, 90, 021802, doi: [10.1103/PhysRevLett.90.021802](https://doi.org/10.1103/PhysRevLett.90.021802)
- Giunti, C., & Studenikin, A. 2015, *Rev. Mod. Phys.*, 87, 531, doi: [10.1103/RevModPhys.87.531](https://doi.org/10.1103/RevModPhys.87.531)
- Giunti, C., & Wook, K. C. 2007, *Fundamentals of Neutrino Physics and Astrophysics* (Oxford: Oxford Univ.), doi: [10.1093/acprof:oso/9780198508717.001.0001](https://doi.org/10.1093/acprof:oso/9780198508717.001.0001)
- González-Reina, O. I., & Vázquez-Jáuregui, E. 2022, Software package for "EstrellaNueva: an open-source software to study the interactions and detection of neutrinos emitted by supernovae", 1, Zenodo, doi: [10.5281/zenodo.6354850](https://doi.org/10.5281/zenodo.6354850)
- Harris, C. R., Millman, K. J., van der Walt, S. J., et al. 2020, *Nature*, 585, 357, doi: [10.1038/s41586-020-2649-2](https://doi.org/10.1038/s41586-020-2649-2)
- Horowitz, C. J., Coakley, K. J., & McKinsey, D. N. 2003, *Phys. Rev. D*, 68, 023005, doi: [10.1103/PhysRevD.68.023005](https://doi.org/10.1103/PhysRevD.68.023005)
- Huber, P., Kopp, J., Lindner, M., Rolinec, M., & Winter, W. 2007, *Computer Physics Communications*, 177, 432, doi: <https://doi.org/10.1016/j.cpc.2007.05.004>
- Huber, P., Lindner, M., & Winter, W. 2005, *Computer Physics Communications*, 167, 195, doi: <https://doi.org/10.1016/j.cpc.2005.01.003>
- Hüdepohl, L., Müller, B., Janka, H.-T., Marek, A., & Raffelt, G. G. 2010, *Phys. Rev. Lett.*, 104, 251101, doi: [10.1103/PhysRevLett.104.251101](https://doi.org/10.1103/PhysRevLett.104.251101)
- Hunter, J. D. 2007, *Computing in Science & Engineering*, 9, 90, doi: [10.1109/MCSE.2007.55](https://doi.org/10.1109/MCSE.2007.55)
- Ikeda, M., Takeda, A., Fukuda, Y., et al. 2007, *The Astrophysical Journal*, 669, 519, doi: [10.1086/521547](https://doi.org/10.1086/521547)
- Janka, H.-T. 2022, *The Garching Core-Collapse Supernova Research*. <https://wwwmpa.mpa-garching.mpg.de/ccsnarchive/>
- Keil, M. T., Raffelt, G. G., & Janka, H.-T. 2003, *The Astrophysical Journal*, 590, 971, doi: [10.1086/375130](https://doi.org/10.1086/375130)
- Lang, R. F., McCabe, C., Reichard, S., Selvi, M., & Tamborra, I. 2016, *Phys. Rev. D*, 94, 103009, doi: [10.1103/PhysRevD.94.103009](https://doi.org/10.1103/PhysRevD.94.103009)
- Lattimer, J. M., & Douglas Swesty, F. 1991, *Nuclear Physics A*, 535, 331, doi: [https://doi.org/10.1016/0375-9474\(91\)90452-C](https://doi.org/10.1016/0375-9474(91)90452-C)
- Lewin, J., & Smith, P. 1996, *Astroparticle Physics*, 6, 87, doi: [https://doi.org/10.1016/S0927-6505\(96\)00047-3](https://doi.org/10.1016/S0927-6505(96)00047-3)
- Liao, J., Liu, H., & Marfatia, D. 2021, *Phys. Rev. D*, 104, 015005, doi: [10.1103/PhysRevD.104.015005](https://doi.org/10.1103/PhysRevD.104.015005)
- Lu, J.-S., Cao, J., Li, Y.-F., & Zhou, S. 2015, *Journal of Cosmology and Astroparticle Physics*, 2015, 044, doi: [10.1088/1475-7516/2015/05/044](https://doi.org/10.1088/1475-7516/2015/05/044)
- Lunardini, C. 2006, *Astropart. Phys.*, 26, 190, doi: [10.1016/j.astropartphys.2006.06.008](https://doi.org/10.1016/j.astropartphys.2006.06.008)

- Migenda, J., Cartwright, S., Kneale, L., et al. 2021, *Journal of Open Source Software*, 6, 2877, doi: [10.21105/joss.02877](https://doi.org/10.21105/joss.02877)
- Mirizzi, A., Tamborra, I., Janka, H.-T., et al. 2016, *Riv. Nuovo Cim.*, 39, 1, doi: [10.1393/ncr/i2016-10120-8](https://doi.org/10.1393/ncr/i2016-10120-8)
- Müller, B., Janka, H.-T., & Dimmelmeier, H. 2010, *The Astrophysical Journal Supplement Series*, 189, 104, doi: [10.1088/0067-0049/189/1/104](https://doi.org/10.1088/0067-0049/189/1/104)
- Papoulias, D., Kosmas, T., Sahu, R., Kota, V., & Hota, M. 2020, *Physics Letters B*, 800, 135133, doi: <https://doi.org/10.1016/j.physletb.2019.135133>
- Scholberg, K., Albert, J., Beck, A., et al. 2020, *SNOwGLOBES: SuperNova Observatories with GLOBES*. <https://github.com/SNOwGLOBES/snowglobes/blob/master/doc/snowglobes.1.2.pdf>
- Serpico, P. D., Chakraborty, S., Fischer, T., et al. 2012, *Phys. Rev. D*, 85, 085031, doi: [10.1103/PhysRevD.85.085031](https://doi.org/10.1103/PhysRevD.85.085031)
- Shen, H., Toki, H., Oyamatsu, K., & Sumiyoshi, K. 1998, *Nuclear Physics A*, 637, 435, doi: [https://doi.org/10.1016/S0375-9474\(98\)00236-X](https://doi.org/10.1016/S0375-9474(98)00236-X)
- Steiner, A. W., Hempel, M., & Fischer, T. 2013, *The Astrophysical Journal*, 774, 17, doi: [10.1088/0004-637x/774/1/17](https://doi.org/10.1088/0004-637x/774/1/17)
- Strumia, A., & Vissani, F. 2003, *Physics Letters B*, 564, 42, doi: [https://doi.org/10.1016/S0370-2693\(03\)00616-6](https://doi.org/10.1016/S0370-2693(03)00616-6)
- Tiesinga, E., Mohr, P. J., Newell, D. B., & Taylor, B. N. 2021, *Rev. Mod. Phys.*, 93, 025010, doi: [10.1103/RevModPhys.93.025010](https://doi.org/10.1103/RevModPhys.93.025010)
- Virtanen, P., Gommers, R., Oliphant, T. E., et al. 2020, *Nature Methods*, 17, 261, doi: [10.1038/s41592-019-0686-2](https://doi.org/10.1038/s41592-019-0686-2)
- Väänänen, D., & Volpe, C. 2011, *Journal of Cosmology and Astroparticle Physics*, 2011, 019, doi: [10.1088/1475-7516/2011/10/019](https://doi.org/10.1088/1475-7516/2011/10/019)
- Xu, J., Huang, M.-Y., Hu, L.-J., Guo, X.-H., & Young, B.-L. 2014, *Communications in Theoretical Physics*, 61, 226, doi: [10.1088/0253-6102/61/2/14](https://doi.org/10.1088/0253-6102/61/2/14)